



Influence of friction stir processing on microstructure and mechanical properties of AA6061 reinforced with Zr and Ni metallic particles

M BALAKRISHNAN^{1,*} , S VIGNESHWARAN², K VINOTHKUMAR²,
EL-SAYED I ABDEL AZIZ³ and MOHAMMAD ABDUR RASHEED⁴

¹Department of Mechanical Engineering, Nehru Institute of Engineering and Technology, Coimbatore 641 105, India

²Department of Mechanical Engineering, SRM Institute of Science and Technology, Ramapuram Campus, Chennai 600 089, India

³Department of Mechanical Engineering, Shaqra University, Dawadmi, Riyadh 11911, Saudi Arabia

⁴Department of Civil Engineering, Shaqra University, Dawadmi, Riyadh 11911, Saudi Arabia

*Author for correspondence (balakrishnn0002@gmail.com)

MS received 30 March 2023; accepted 25 November 2023

Abstract. Friction stir processing (FSP) is considered as a prolific secondary processing method to enhance the properties of aluminium matrix composites (AMCs) by altering their microstructure. AA6061/(15 wt.%) Al₃Zr and AA6061/(15 wt.%) Al₃Ni AMCs were manufactured with the addition of zirconium (Zr) and nickel (Ni) powders to the molten AA6061 and followed by FSP. The change in microstructure of AMCs before and after FSP was analysed through optical and electron microscopies integrated with electron back-scattered diffraction. The cast AMCs exhibited clustered, sharp cornered particles with micropores near the particle–matrix interfaces and showed coarse-grained microstructure. Upon conducting FSP, the particle distribution was uniform along with the elimination of cast defects. The sharp cornered particles were fragmented into finely dispersed particles in the aluminium matrix. Significant grain refinement was observed on AMCs owing to the pinning effect of particles and severe deformation happened during FSP. FSP enhanced the accumulation of dislocations and resulted in modification microstructure, which favoured attaining a combination of ductility and tensile strength. The strength attained by the Al₃Ni AMC was higher than that of Al₃Zr AMC due to the existence of finely dispersed near round-shaped particles, which exhibited better load-bearing ability.

Keywords. Aluminium matrix composites; friction stir processing; microstructure; tensile strength; intermetallic particles; casting.

1. Introduction

The aluminium matrix composites (AMCs) are treated as one of the viable materials due to its high specific strength, thermal stability and wear resistance properties [1]. Product manufacturers in various sectors constantly search for materials, which have excellent strength-to-weight ratios [2]. AMCs produced through liquid state processes and powder metallurgical routes with a wide range of ceramic reinforcement particles are challenging due to poor wettability and agglomeration of ceramic particles, which eventually deteriorate the mechanical properties [3]. Besides, it is even more challenging to fabricate metal matrix composites (MMCs) with nano-sized reinforcement particles as the surface area increases for the given volume fraction of micron-sized reinforcement particles [4]. Improved tensile strength at the expense of ductility is attributed to poor deformation behaviour in the case of ceramic-reinforced AMCs [5]. AMCs fabricated with intermetallic particles are

suitable enough when compared to the challenges faced during reinforcing ceramic particles. Moreover, AMCs with intermetallic particles like Al₃Ti, Al₃C4, Al₃Fe and Al₃Cu reveal high wettability and their physical and thermal properties are close to that of aluminium alloys. Hence, proper interfacial bonding occurs between the matrix and reinforcement [6]. The fabrication of Al-based AMCs reinforced with Al₃Zr [7, 8] and Al₃Ni [9, 10] using various manufacturing methods is well documented in the literature. Particles like Al₃Zr and Al₃Ni in Al matrix are successful and also they enhance the hardness and wear resistance ability of AMCs. Irrespective of the homogeneous distribution of Al₃Zr and Al₃Ni in the Al matrix, the attained tensile properties are inferior due to certain undesirable features like segregation of particles within grain boundaries, agglomeration, formation of pores and high aspect ratio of polygonal-shaped particles. To overcome the aforesaid challenge, it is essential to modify the shape and size factors as well as the distribution of *in situ* Al₃Zr

particles to gain high strength. Hence, the primary cast AMCs are subjected to additional processing methods like rolling, extrusion and forging [11–13]. Additional processing methods improve the tensile strength; however, they do not alter the distribution as there is no complete plasticized material flow in all directions. To overcome this, friction stir processing (FSP) evolved as a prolific method for the better distribution of reinforcement particles in AMCs [14]. During FSP, the plunged rotating tool causes plastic deformation in the material due to the tool action and frictional heat influence. Further, the strain induced on the material during FSP is higher than any other conventional secondary processing routes [15]. Utilizing the FSP, the refined morphology and well-distributed AMCs have been produced using various reinforcement particles, namely Al_2O_3 [16], TiB_2 [17], SiC [18], Al_3Zr and Al_3Ti [19].

There are only a few reports on the FSP of cast Al with Al_3Zr and Al_3Ni for the production of AMCs. The present study focusses as on FSP of Al matrix reinforced with 15 wt.% of Zr and Ni that evolved as Al_3Zr and Al_3Ni using an *in situ* reaction between Al matrix and Zr and Ni powders. The structure–property studies were conducted in detail.

2. Experimental

The investigated material AA6061 was procured in the form of 30-mm diameter solid rods and the temper condition of the as-procured rod was in T6. The chemical composition of the investigated material acquired through X-ray fluorescence is (in wt.%) 0.01 Ti, 0.02 Ni, 0.08 Zn, 0.09 Cr, 0.13 Mn, 0.17 Cu, 0.22 Fe, 0.54 Si, 0.95 Mg and the remainder is aluminium. A computed number of rods, which are sufficient to fill the mould cavity was melted using an electric resistance furnace. The estimated quantities of Zr and Ni powders were added to two different molten aluminium to initiate the chemical reaction. To restrict the formation of slags, the volume fraction of Zr and Ni was fixed to 15 wt.%. The morphology of the as-procured Zr and Ni powders is shown in figure 1a, b. In the furnace, the molten

AA6061 was kept at a temperature of 850°C for 45 min. For the homogeneous distribution of particles, periodical agitation of the aluminium melt was carried out. Furthermore, the melt was transferred to the permanent moulds and the final castings were obtained with a dimension of 100 × 100 × 20 mm. As a result, two different cast slabs of AA6061 with 15 wt.% of Zr and Ni reinforcements were obtained and the same were wire-cut to 100 × 50 × 8 mm using an electric discharge machine (EDM). FSP was conducted on the wire-cut plates using a computer numerical controlled vertical milling centre. The tool rotational speed of 1200 rpm, traverse speed of 50 mm min⁻¹, tool tilt angle of 0°, shoulder diameter of 18 mm, pin diameter of 6 mm, pin length of 5.7 mm, number of FSP passes as two and by using HCHCr tool, steel with hexagonal shape tool were considered to be the FSP process parameters as per the earlier report of Rajan *et al* [20].

Microscopic examinations were carried out for the specimens that were sliced from the cast slab and friction stir processed plates. For recording the optical micrographs, the aforesaid specimens were mounted (STRUERS™ Citropress 5) and mechanically polished (STRUERS™ Labopol 25). Using Keller's (2.5 ml of HNO_3 , 1.5 ml of HCl, 1 ml of HF and 95 ml of distilled water) reagent, the etched surface was observed using a light optical microscope (OLYMPUS™ BX51 M) and a field emission scanning electron microscope (FESEM, CARL ZEISS™-SIGMAHV). For the electron backscattered diffraction (EBSD), the samples were polished using grit papers, such as 100, 1000 and 5000. Besides, diamond polishing and colloidal polishing (in 100 μm suspension) were executed. Later, samples were electro-polished (STRUERS™-Electropol-IV) in an electrolytic bath containing 20% perchloric acid and 80% methanol at −16°C with an operating voltage of 16 V for 20 s. FEI™ Quanta-3D FESEM was used for recording the EBSD images integrated with TSL-OIM™ software [21]. Finer microstructural details were obtained using JEOL™ JEM 2100 high-resolution transmission electron microscope (HRTEM). The samples were ion polished (GATAN™) using a precision ion polishing unit

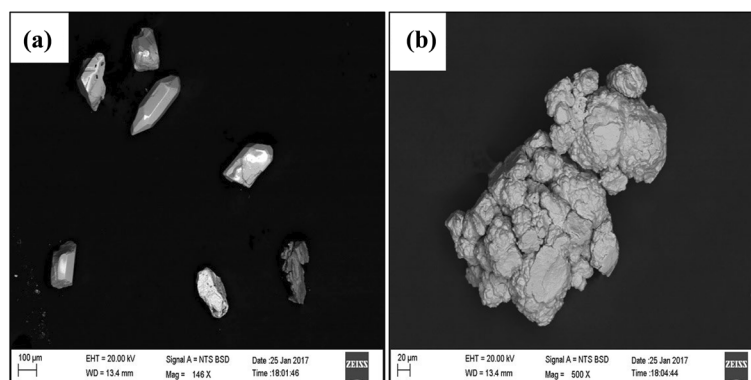


Figure 1. FESEM micrograph of as-received reinforcement particles: (a) zirconium and (b) nickel.

and the operating voltage of HRTEM was fixed as 200 kV for the observation. X-ray diffraction (XRD) was recorded using Rigaku Ultima IIITM with the aid of CuK α radiation. The wavelength of the radiation was 1.54 Å with a step size of 2° min⁻¹.

Tensile specimens prepared from the cast slab had a gauge length of 40 mm, width of 7 mm and thickness of 6 mm. After FSP, the tensile specimens with a gauge length of 30 mm, width and thickness of 4 mm were wire-cut from the stir zone using an EDM. The ultimate tensile strength (UTS) was estimated from INSTRONTM 1195 tensile test unit at a strain rate of 0.5 mm s⁻¹. An average of five readings was considered as UTS value. The fracture surface morphology of the failed tensile specimens was obtained using the FESEM unit.

3. Results and discussion

3.1 XRD analysis

XRD peaks of as-procured AA6061 and AA6061 processed with 15 wt.% of Zr and Ni aluminium matrix composite (AMCs) are shown in figure 2. The peaks of the matrix (aluminium) and reinforcement phases (Al₃Zr and Al₃Ni) are detected after FSP. The presence of Al₃Zr and Al₃Ni peaks ensures the formation of intermetallic phases due to the chemical reaction between aluminium–zirconium and

aluminium–nickel at a higher temperature. The formation of intermetallic phases occurs as per the following equations:



No separate Zr and Ni peaks are identified in the XRD diffractogram (see figure 2). This is attributed to the complete dissolution of Zr and Ni in the AA6061 matrix during the chemical reaction and the holding time period, which resulted in total consumption of elements. Furthermore, there was no other formation of compounds like AlZr, Al₃Zr₂, Al₃Zr₄ and Al₂Zr₃ [22, 23] in the case of AA6061–Zr combination. Similarly, the formation of compounds like AlNi, Al₃Ni₅, Al₃Ni₂ and AlNi₃ [24, 25] are not identified in the AA6061–Ni combination. This could be possibly due to the lower free energy of formation of Al₃Zr and Al₃Ni phases or because of a lack of sufficient quantity of Zr and Ni powders during the reaction. The non-existence of other compounds clearly indicates that the Al₃Zr and Al₃Ni were highly stable at the time of reaction and did not form into other compounds through decomposition.

3.2 Microstructure

Microstructures of as-cast AA6061 and AA6061 reinforced with 15 wt.% Zr and Ni in cast and friction stir processed condition are depicted as the optical and FESEM micrographs in figures 3 and 4, respectively. The micrograph reveals variation in the microstructure as a function of FSP on two different AMCs exhibiting Al₃Zr and Al₃Ni intermetallics. The as-cast AA6061 without the addition of any reinforcement particles shows a clear dendritic microstructure (refer to the longer arm structure in figures 3a and 4a), which is common in cast products. In the process of solidification, the cooling rate is sufficient enough to produce the dendritic structure. In the case of AMC, the presence of Al₃Zr reduced the formation of cast microstructure (fewer dendrites) and a considerable volume of Al₃Zr particles are observed in the AA6061 matrix as seen in figures 3b and 4b, respectively. Furthermore, the distribution of Al₃Zr particles is inhomogeneous and the particles show sharp edges with traces of micropores between the AA6061 matrix and Al₃Zr particles (refer to figure 3b). However, AMC fabricated with Al₃Ni particles has completely altered the cast microstructure because of the solidification pattern. Besides, the dendritic structure is completely refined with no traces of initial cast structure as observed in figures 3c and 4c. Apart from the near homogeneous distribution of Al₃Ni particles in the AA6061 matrix, there are clustering and segregation of particles along with the formation of micropores between matrix particle interfaces. The formation of pores is an indication of poor interfacial bonding between the matrix and reinforcement. Firstly, the homogeneous distribution of

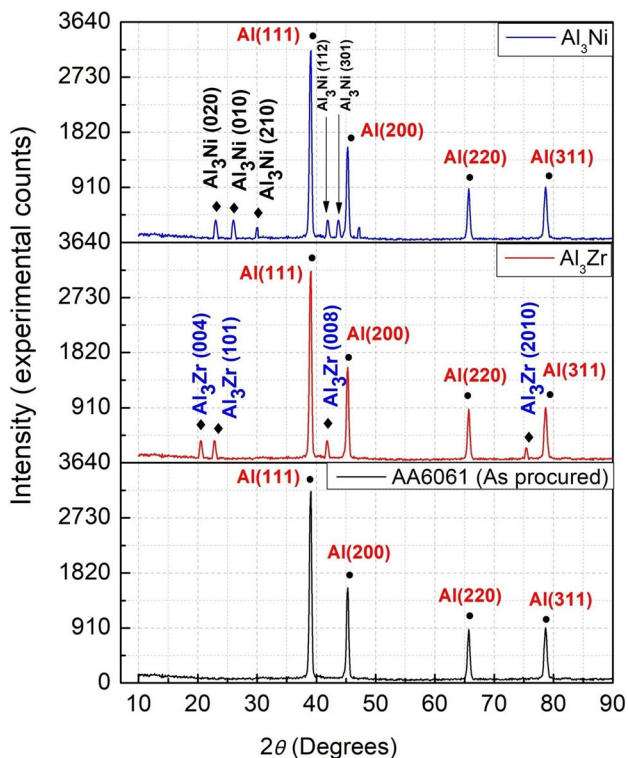


Figure 2. XRD diffractogram of as-procured AA6061 and AA6061 reinforced with 15 wt.% of Al₃Zr and Al₃Ni.

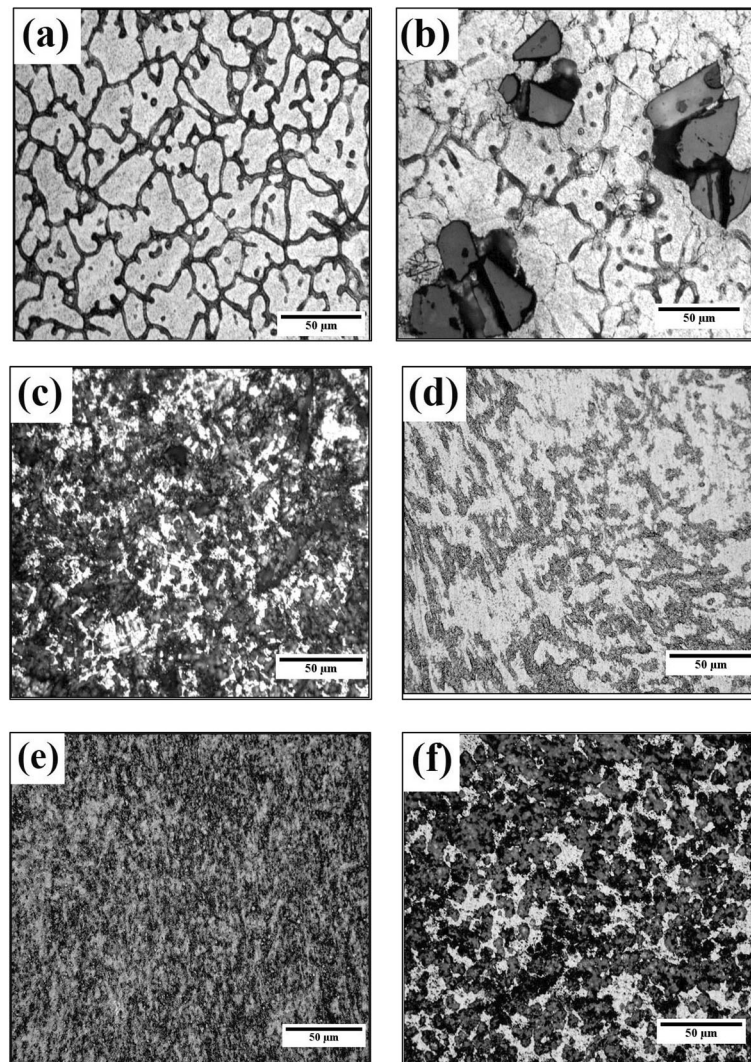


Figure 3. Optical micrograph images of AA6061 AMCs in cast condition: (a) as-cast BM, cast with: (b) 15 wt.% Zr showing Al_3Zr , (c) 15 wt.% Ni showing Al_3Ni , (d) BM friction stir processed, friction stir processed with: (e) 15 wt.% Zr showing Al_3Zr and (f) 15 wt.% Ni showing Al_3Ni .

reinforcement particle depends on the retention time before pouring into the moulding cavity and solidification pattern. Secondly, the pace of solidification front also decides the distribution of particles. According to Sasikumar and Kumar [26] the two possibilities are related to the pace of solidification front. If the pace of solidification front is greater than the critical value, the distribution of particles will be in the grain boundaries. Else, the particle distribution will be segregated surrounding the grain boundaries. In the present study, the microstructure suggests that the particles (Al_3Zr and Al_3Ni) were propelled along with the solidification front and since the particle size is larger, the microstructure does not reveal any segregation along the grain boundaries. Hence, the propelled-up particles show a clustered pattern with a non-uniform distribution. The pores

observed near the particle–matrix interface could be due to high cooling rates that would have prevented the release of entrapped gases during cooling. The formation of clusters and micropores tend to decrease the tensile properties of the fabricated AMCs. It is recommended to reformulate the microstructure, which is favourable for the betterment of tensile properties.

In this study, to improve the tensile properties of fabricated AMCs, it was proposed to conduct FSP. The microstructure of AA6061 without any reinforcement particle after the FSP is shown in the optical and SEM micrographs, depicted in figures 3d and 4d, respectively. However, the microstructure of AMCs fabricated using AA6061 with 15wt.% Zr and Ni subjected to FSP are shown in the optical and SEM micrographs (figures 3e–f and 4e–f). The microstructure after the

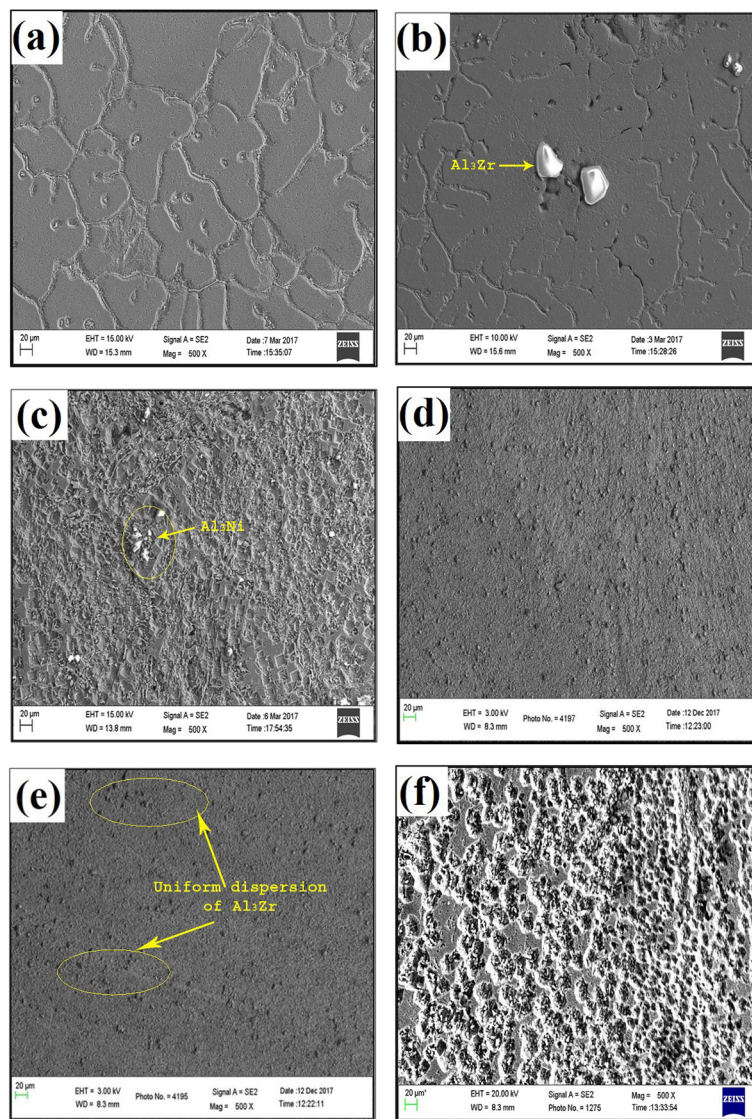


Figure 4. FESEM microstructure of AA6061 AMCs in cast condition: (a) as-cast BM, cast with: (b) 15 wt.% Zr showing Al_3Zr , (c) 15 wt.% Ni showing Al_3Ni , (d) BM friction stir processed, friction stir processed with: (e) 15 wt.% Zr showing Al_3Zr and (f) 15 wt.% Ni showing Al_3Ni .

FSP process shows significant evolution with no traces of its earlier cast microstructure as observed in figure 5a and the FSP mechanism involving grain refinement is displayed in figure 5b. The deformation that takes place during FSP results in a modified refined microstructure as observed in figures 3d and 4d. Also, the micrographs shown in figures 3e–f and 4e–f indicate an uniform distribution of reinforcement particles (Al_3Zr and Al_3Ni) in the AA6061 matrix. The shape and size of reinforcement particles also reveal significant changes when compared to the reinforcement particles in the cast AMCs. Besides, the microstructure of AMCs subjected to FSP shows no clustering of particles as well as there are no pore formations. The determining factors involved in the conversion of original cast microstructure during FSP are

manifested below. The AA6061 matrix metal was plasticized, which is attributed to the influence of frictional heat produced by the rotating tool and caused a complicated flow owing to the tool force and plate movement. The flow of material occurs in a three-dimensional direction within the available space between the tool and parent composite. However, in the case of other deformation processes, a similar trend of three-dimensional material flow is not possible. At the time of FSP, the plasticized matrix metal moves over the tool pin several times before the consolidation at the rear end of the tool [27]. Also, the shape of the tool causes bobbing action in the direction of thickness of the plate. The reinforcement particles (Al_3Zr and Al_3Ni) do not plasticize like the matrix metal. The plasticized matrix metal moves rapidly to that of

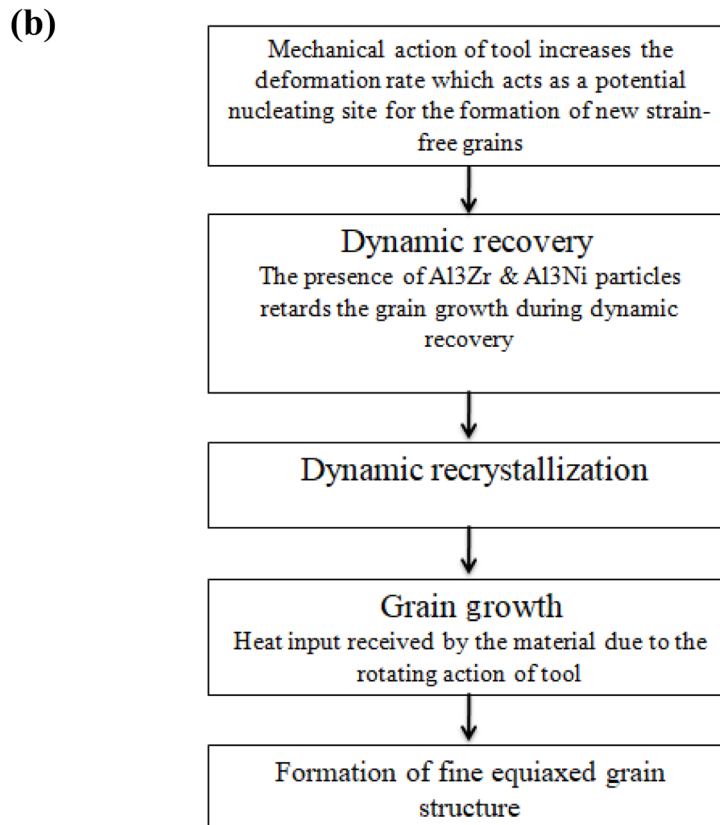
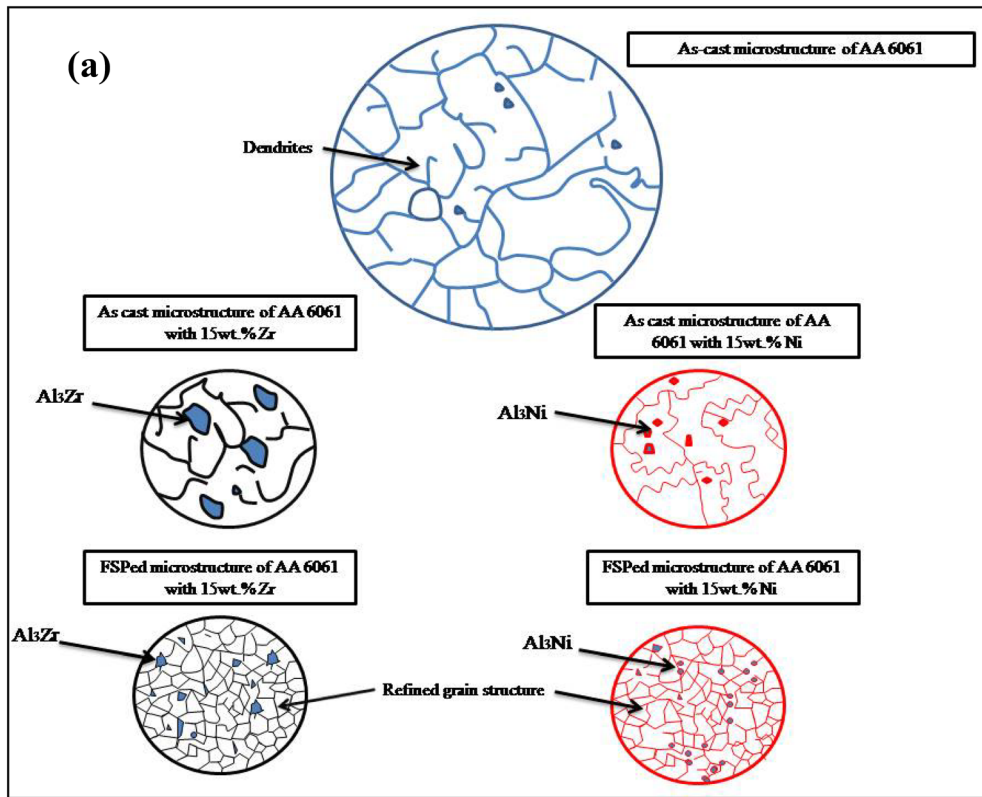


Figure 5. (a) Schematic transformation of microstructure. (b) Mechanism of grain refinement in FSP.

reinforcement particles. The rapidly moving matrix metal distinguishes the clustered particles and scatters them. This results in the homogeneous distribution of reinforcement particles in the AA6061 matrix. The frictional heat is not sufficient enough to melt the AA6061 matrix, which suppresses the effect of solidification on particle distribution. After the FSP, the AMCs cool and consolidation occur, which restrict the particle movement in the matrix. The deformation strain faced by the particles in the AMCs is higher, which leads to particle breakdown. This in turn causes fine dispersion of fragmented particles in the AA6061 matrix as observed in figures 3e–f and 4e–f. Similar observations were reported by various researchers on preparing surface composites using FSP [15]. Moreover, the fast-rotating action of the FSP tool blends the fragmented particles in the AA6061 matrix. The sharp edges of the particles turn blunt or become round owing to the abrading action of the FSP tool [28]. The stress attributed to the lateral material flow becomes favourable to enhance the particle morphology. The mixing and vertical force during FSP eradicate the micropores in the AMCs. The micrographs shown in figures 3–4 prove that FSP is one of the prolific methods to alter the initial microstructure to a favourable one.

3.3 Mechanical properties and fractography

The ultimate tensile strength (UTS) values of the AA6061 base metal, AMCs and AMCs subjected to FSP are presented in figure 6. The evolution of Al₃Zr in the AMC reinforced with Zr particles and the emergence of Al₃Ni in the AMC reinforced with Ni particles resulted in a composite strengthening. The UTS of base metal shows a value

of 152 MPa, whereas the UTS of AMC with Zr particles reveals 112 MPa. However, AMC with Ni particles notifies 209 MPa as UTS. This indicates that there is no improvement in the strength values due to the evolution of Al₃Zr particles. This could be due to the formation of Al₃Zr clusters and during tensile deformation, the clusters will tear-off instead of taking the load. Also, the bonding strength of clusters with the matrix metal is low. Moreover, the large platelet-shaped Al₃Zr particle has the tendency to break and creates a lag in the load transferring capacity. In addition, the pores observed in the SEM microstructure, reduced the cross-sectional area to support the tensile deformation. Further, these pores would have acted as stress concentrators during the tensile test, which showed relatively lesser tensile strength than that of the as-cast AA6061 base metal. In the case of AMC reinforced with Ni particle showed significant improvement in tensile strength when compared to the base metal. The increase in strength is attributed to grain boundary strengthening. Also, during the tensile deformation, the applied load has the possibility to be moved to harder Al₃Ni particles across the aluminium matrix. The formation of strain fields due to the variation in the coefficient of thermal expansion retards the dislocation movement. Significant improvement in strength is noted in AMCs after FSP. The base metal subjected to FSP showed a value of 192 MPa as tensile strength. However, the AMC with Zr particle subjected to FSP shows 265 MPa and the AMC with Ni particle subjected to FSP identifies 325 MPa as tensile strength values. This improvement in strength is due to the redistribution of Al₃Zr and Al₃Ni particles in the AA6061 matrix causes Orowan strengthening due to uniform distribution [29]. After the FSP, due to the betterment in the interfacial bonding between the particles and matrix metal, the load transferability of the AMCs was observed to be better during the tensile deformation. The grain refinement strengthened the AMCs predominantly. Also, micropores observed in the cast AMCs closed after the FSP and provided a higher area to resist the tensile deformation. Apart from grain boundary strengthening, the deformation also induced the formation of dislocations and promoted dislocation-based strengthening, which resulted in the improvement of tensile strength [30].

The fracture surface morphology of the fractured tensile specimen for the base metal, AMCs and AMCs subjected to FSP are provided in figure 7a–f. The cast base metal and AMCs show no formation of dimples and the fractured surface is viewed to be flat with some pores. This is a typical indication of a brittle mode of failure and there is no proof for the occurrence of plastic flow of material before failure. Moreover, the fracture surface morphology of AMCs subjected to FSP show dimples with clear evidence of plastic flow before the failure. This indicates the ductile phenomenon of failure in the AMCs subjected to FSP. As FSP promotes uniform distribution of particles and eliminates pores. This improved the ductility after FSP.

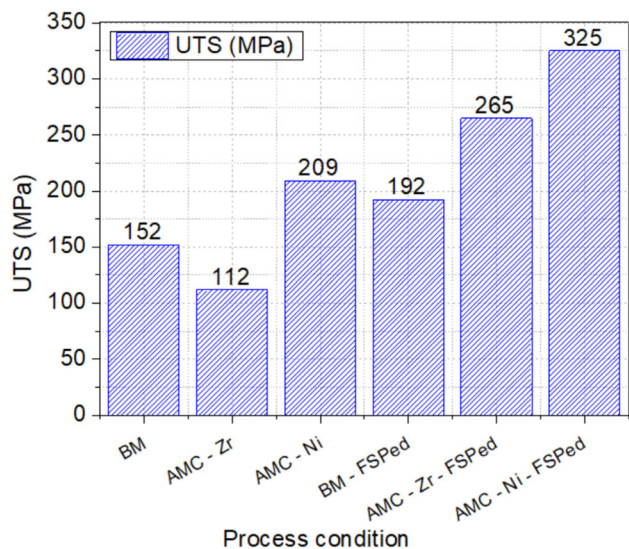


Figure 6. Effect of reinforcement addition and fraction stir processing on the tensile strength of AA6061/Al₃Zr and AA6061/Al₃Ni AMCs.

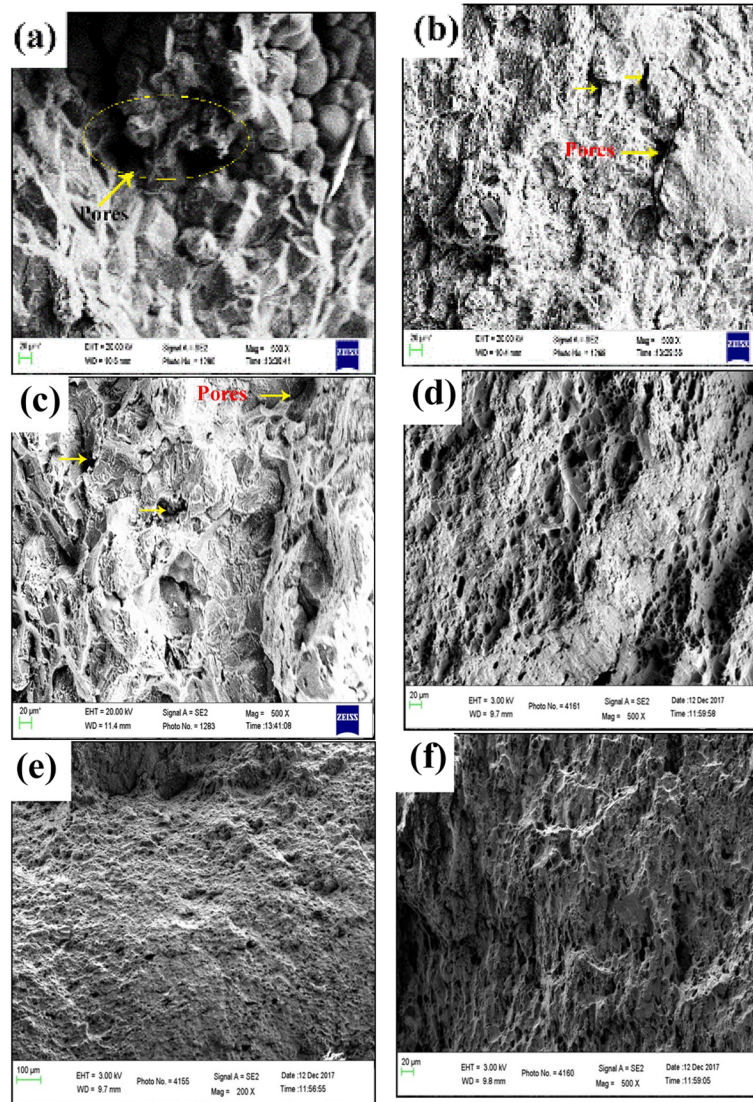


Figure 7. FESEM fracture surface morphology of AA6061 AMCs in cast condition: (a) as-cast BM, cast with: (b) 15 wt.% Zr, (c) 15 wt.% Ni, (d) BM friction stir processed, friction stir processed with: (e) 15 wt.% Zr and (f) 15 wt.% Ni.

4. Conclusions

FSP resulted in particle redistribution, which caused a uniform distribution attributed to the three-dimensional material flow, also supported by the stirring action of the FSP tool. FSP fragmented the platelet and polygonal-shaped Al_3Zr and Al_3Ni particles. After FSP, the particles turned fine with round edges due to the severe deformation caused by the rotating tool. FSP modified the cast microstructure and assisted in the closure of micropores because of plasticized material flow. FSP refined the grain size of AMCs by dynamic recrystallization, which resulted due to frictional heat and deformation. Along with grain refinement, FSP accumulated the dislocations due to thermal mismatch of particle–matrix and plastic deformation. FSP enhanced the

tensile strength of the AMCs attributed to the change in microstructure. The fracture surface of the AMCs subjected to FSP validates the ductile mode of failure.

Acknowledgements

We are thankful to the Centre for Research in Metallurgy, Karunya University, M/s Vigshan tools and Speed Spark EDM at Coimbatore, Microscopy Lab at University of Johannesburg, FESEM lab at Coimbatore Institute of Technology, The South India Textile Research Association (SITRA) at Coimbatore, OIM and Texture Lab at Indian Institute of Technology Bombay and PSG Institute of

Advanced Studies for providing the facilities to carry out this investigation.

References

- [1] Adesina A Y, Al-Badour F A and Gasem Z M 2018 *J. Manuf. Process.* **33** 111
- [2] Huang G and Shen Y 2017 *J. Manuf. Process.* **30** 361
- [3] Arunachalam R, Krishnan P K and Muraliraja R 2019 *J. Manuf. Process.* **42** 213
- [4] Harichandran R and Selvakumar N 2016 *Arch. Civ. Mech. Eng.* **16** 147
- [5] Chen Z Y, Chen Y Y, Shu Q, An G Y, Li D and Liu Y Y 2000 *Metall. Mater. Trans. A* **31** 1959
- [6] Gangil N, Siddiquee A N and Maheshwari S 2017 *J. Alloys Compd.* **715** 91
- [7] El-Hadada S, Sato H and Watanabe Y 2010 *J. Mater. Process. Technol.* **210** 2245
- [8] Kaveendran B, Wang G S, Huang L J, Geng L and Peng H X 2018 *J. Alloys Compd.* **581** 16
- [9] Rajan T P D, Pillai R M and Pai B C 2008 *J. Alloys Compd.* **4** 534
- [10] Choi Y B, Matsugi K and Sasaki G 2022 *J. Compos. Mater.* **48** 2289
- [11] Ahmed S, Ahsan Q and Kurny A S W 2007 *J. Mater. Process. Technol.* **182** 327
- [12] Zamani R, Mirzadeh H and Emamy M 2018 *Mater. Sci. Eng. A* **726** 10
- [13] Kapoor R, Sarkar A, Behera A N and Sunil S 2020 *Mater. Sci. Eng. A* **772** 138805
- [14] Ma Z Y 2008 *Metall. Mater. Trans. A* **39** 642
- [15] Sharma V, Prakash U and Manoj Kumar B V 2015 *J. Mater. Process. Technol.* **224** 117
- [16] Hoziefa W, Toschi S, Ahmed M M Z, Morri A, Mahdy A A, Seleman M M E *et al* 2016 *Mater. Des.* **106** 273
- [17] Yadav D and Bauri R 2015 *J. Mater. Eng. Perform.* **24** 1116
- [18] Vijayavel P, Balasubramanian V and Sundaram S 2014 *Mater. Des.* **57** 1
- [19] Dinaharan I, Ashok Kumar G, Vijay S J and Murugan N 2014 *Mater. Des.* **63** 213
- [20] Michael Rajan H B, Dinaharan I, Ramabalan S and Akinlabi E T 2016 *J. Alloys Compd.* **657** 250
- [21] Vigneshwaran S, Sivaprasad K, Narayanasamy R and Venkateswarlu K 2019 *Metall. Mater. Trans. A* **50** 3281
- [22] Duan Y H, Huang B, Sun Y, Peng M J and Zhou S G 2014 *J. Alloys Compd.* **590** 50
- [23] Du J, Wen B, Melnik R and Kawazoe Y 2015 *Comput. Mater. Sci.* **103** 170
- [24] Wen Z, Zhao Y, Hou H, Tian J and Han P 2017 *Superlattices Microstruct.* **103** 9
- [25] Kim J T, Hong S H, Park J M, Eckert J and Kim K B 2018 *J. Alloys Compd.* **749** 205
- [26] Sasikumar R and Kumar M 1991 *Acta Metall. Mater.* **39** 2503
- [27] Zhao Y H, Lin S B, Qu F X and Wu L 2006 *Mater. Sci. Technol.* **22** 45
- [28] Prater T 2011 *Mater. Manuf. Process.* **26** 636
- [29] Queyreau S, Monnet G and Devincere B 2010 *Acta Mater.* **58** 5586
- [30] Gautam G, Kumar N, Mohan A, Gautam R K and Mohan S 2016 *J. Compos. Mater.* **504** 123

Springer Nature or its licensor (e.g. a society or other partner) holds exclusive rights to this article under a publishing agreement with the author(s) or other rightsholder(s); author self-archiving of the accepted manuscript version of this article is solely governed by the terms of such publishing agreement and applicable law.